Journal of Nuclear Materials 386–388 (2009) 529–532

Contents lists available at ScienceDirect

Journal of Nuclear Materials

journal homepage: www.elsevier.com/locate/jnucmat

Cyclically induced softening in reduced activation ferritic/martensitic steel before and after neutron irradiation

S.W. Kim [a,b,*], H. Tanigawa [c], T. Hirose [c], A. Kohayama [d]

[a] Graduate School of Energy Science, Kyoto University, Gokasho, Uji, Kyoto 611-0011, Japan
[b] Japan Atomic Energy Agency, 4002 Narita, O-arai, Ibaraki 311-1393, Japan
[c] Japan Atomic Energy Agency, 2-4 Shirakata-Shirane, Tokai, Ibaraki 319-1195, Japan
[d] Institute of Advanced Energy Kyoto University, Gokasho, Uji, Kyoto 611-0011, Japan

A B S T R A C T

Low-cycle fatigue results at ambient temperature under diametral strain-controlled conditions of the reduced activation ferritic/martensitic steel, F82H IEA heat before and after neutron irradiated samples are reported. The results show that cyclic softening behavior is the main mechanical feature observed in this material. A detailed analysis for the hysteresis loops was carried out to determine the friction and back stresses. The friction stress is equivalent to the resistance which the dislocations have to overcome to keep moving in the lattice. The back stress depends on the density of long-range impenetrable obstacles that are created by the dislocations movement such as pile-ups. The cyclic softening of F82H IEA heat is related with the decrease of the friction stress. Moreover, the friction and back stress behavior of neutron irradiated samples show significantly different behavior than those of unirradiated samples.

1. Introduction

In the R&D of ITER test blanket module (TBM) to obtain the data for the DEMO blanket design, reduced activation ferritic/martensitic (RAF/M) steel has been recognized as a primary near-term candidate material [1]. In materials life decision for a commercial blanket (creep-), fatigue property of materials is a particularly important because oscillating temperature gradients, depending on the pulse lengths, the operating conditions, and the thermal conductivities, will cause elastic and elastic-plastic cyclic deformation giving rise to (creep-) fatigue in structural first wall and blanket components [2]. The existing data bases of RAF/M steel provide baseline data set including post-irradiation fatigue data. However, in order to perform the accurate fatigue lifetime assessment for ITER-TBM and beyond utilizing the existing data base, it is mandatory to understand the mechanisms of fatigue fracture. The RAF/M steel, F82H IEA heat has particularly good strength properties with adequate ductility [3]. Much of this performance is based on high dislocation densities and a fine, well dispersed precipitate distribution. F82H IEA heat, however, has an inclination to softening during cyclic loading [4]. Cyclic straining processes can lead to microstructural changes causing cyclic softening of the material. This effect could become a significant engineering problem affecting (creep-) fatigue, swelling and segregation phenomena during irradiation.

It has been previously reported [5,6] that alternating strain destroys the lath structure and induces polygonization, and crack initiation occurs as the final phase of polygonization. And also, irradiation hardening causes a decrease in the strain range, and a size reduction of polygonized regions. The main purpose of the present study is to evaluate the low-cycle fatigue life and the cyclic stress response of normalized and tempered F82H IEA heat at room temperature. The influence of neutron irradiation on the fatigue life and the cyclic stress response was also evaluated.

2. Experimental procedure

The material used was Japanese RAF/M steel, F82H IEA heat, which was normalized at 1313 K for 38–40 min followed by air-cooling (AC) and tempered at 1023 K for 60 min followed by AC. Further details information on this steel can be found elsewhere [3].

Neutron irradiations up to a fluence of 3×10^{19} N/cm^2 ($E > 1.0$ MeV; about 0.02 dpa) at temperatures around 423 K and 573 K were carried out on SF-1 miniaturized hourglass-shaped fatigue specimens [5,6] in the Japan materials testing reactor (JMTR) at Japan Atomic Energy Agency (JAEA). Fig. 1 shows the Vickers hardness distribution of as-prepared and irradiated samples. It can be considered that the low-temperature irradiation caused irradiation hardening.

* Corresponding author. Address: Graduate School of Energy Science, Kyoto University, Gokasho, Uji, Kyoto 611-0011, Japan. Tel.: +81 29 267 3713; fax: +81 29 267 7173.
E-mail address: kimsawoong@gmail.com (S.W. Kim).

0022-3115/$ - see front matter
doi:10.1016/j.jnucmat.2008.12.168

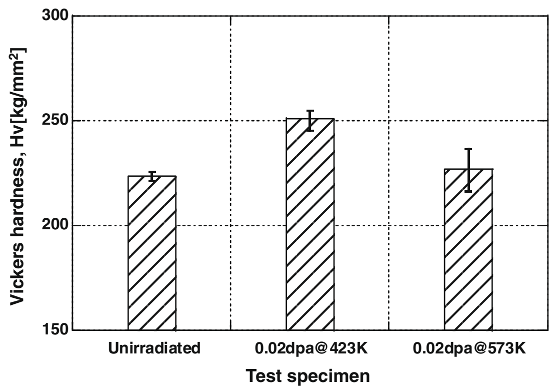

Fig. 1. Vickers hardness distribution of F82H IEA heat before and after irradiation.

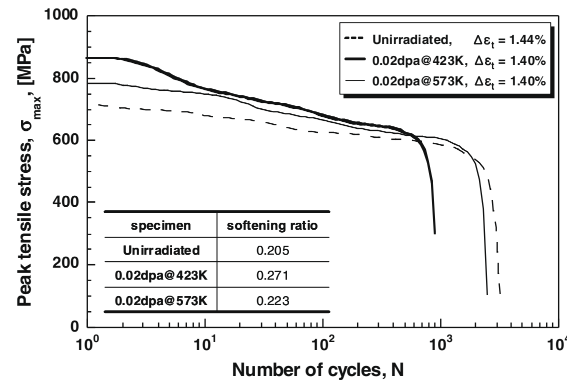

Fig. 3. Evolution of the peak tensile stress during LCF testing of F82H IEA heat before and after irradiation.

Diametral strain-controlled low-cycle fatigue tests were carried out with a triangular strain waveform at ambient temperature, and a total diametral strain range, $\Delta\varepsilon_d$, of 0.4–1.0% based on ASTM standard E-606 [7].

3. Results and discussion

3.1. Low-cycle fatigue properties

The number of cycles to failure, N_f, is plotted against the total strain range, $\Delta\varepsilon_t$, obtained by low-cycle fatigue (LCF) test with unirradiated samples and irradiated at 423 K and 573 K samples in Fig. 2. In all conditions, comparing those results obtained from the LCF tests, it is clear that the fatigue lifetimes in irradiated samples at 423 K decrease significantly than those of unirradiated samples, although the fatigue lifetimes in irradiated samples at 573 K slightly decrease than those of unirradiated samples. This corresponds to hardening caused by low-temperature irradiation.

3.2. Cyclic softening

The cyclic stress response of a material represents an evolution of peak tensile stress with the number of cycles during LCF deformation and is consequence of the interaction between competing mechanisms of hardening and softening. Hence, it is important to figure out which mechanisms are activated for cyclic hardening of softening in order to analyze cyclic stress response of each material. In Fig. 3, the peak tensile stresses, σ_{max} are plotted as a function of number of cycles, N both for unirradiated and two irradiated samples under the controlled strain range about 1.4%. The curve which describes the reduction of peak tensile stress up to failure during the strain-controlled LCF test is called the fatigue softening curve. From those curves, it is noticed that cyclic softening dominated during the strain-controlled LCF test of unirradiated and irradiated samples tested at room temperature. And also, obviously irradiation hardening occurs in initial regions of LCF testing because the initial peak tensile stress of irradiated sample is significantly higher than that of unirradiated sample.

The parameter, 'softening ratio', is introduced to quantify the amount of cyclic softening during LCF deformation and to study its irradiation effect more systematically. Softening ratio is defined in Eq. (1), where σ_{max} and $\sigma_{max}|N_f/2$ are the maximum peak tensile stress and a peak tensile stress at half-life, respectively

$$\text{Softening ratio} = \frac{\sigma_{max} - \sigma_{max|N_f/2}}{\sigma_{max}}. \tag{1}$$

The variation of softening ratio for unirradiated and irradiated samples is presented in Fig. 3. Regarding the change of softening ratio in each sample, the softening ratio increase in order of irradiated sample at 573 K, irradiated sample at 423 K and unirradiated sample. Therefore, it can be considered that the neutron irradiation cause irradiation hardening and significant increase in cyclic softening ratio. According to the results, the fatigue lifetimes of an irradiated sample should be shorter than unirradiated sample.

The cyclic stress response curve (Fig. 3) can be represented as shown in Fig. 4 in order to analyze cyclic softening behavior of unirradiated and irradiated samples more easily. The vertical axis represents the peak tensile stress normalized by initial peak tensile stress, and horizontal axis represents the number of cycles normalized by the number of cycles to failure. The peak tensile stress of the saturated region decreases in the irradiated samples. Though the saturated region can be recognized on softening curves for

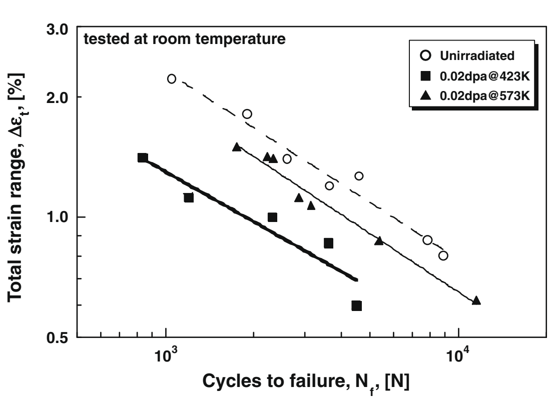

Fig. 2. Low-cycle fatigue life in F82H IEA heat before and after irradiation.

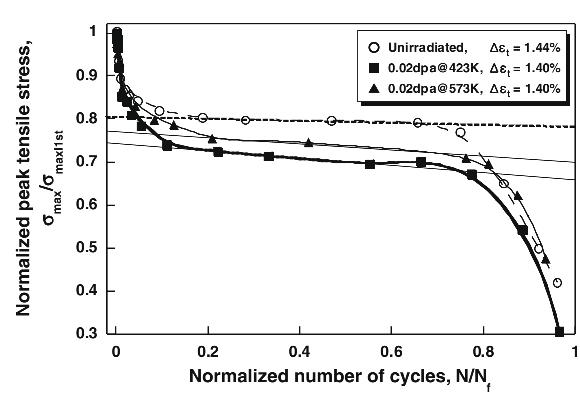

Fig. 4. Cyclic stress response curves of F82H IEA heat before and after irradiation.

unirradiated sample, irradiated samples show continuous softening without any saturated region.

Fatigue softening is a typical phenomenon for materials hardened by precipitation, solid solution, presence of foreign particles and/or martensitic transformation [8]. Fatigue softening is caused by the gradual elimination of obstacles, such as precipitates, foreign particles and grain or lath boundaries, to the motion of dislocations. Although fatigue softening curves usually have a saturated region, the curves for irradiated samples in Fig. 4 did not show any saturation. It can be noticed that change of the distribution and morphology of obstacles continuously occurred.

A detailed analysis of the flow stress, as originally suggested by Cottrell [9] and employed by Kuhlmann-Wilsdorf and Laird [10] as well as Handfield and Dickson [11], was used to determine the mechanisms responsible for the cyclic softening behavior. Upon this method, the flow stress obtained from the hysteresis loops is the result of two kinds of resistance to plastic deformation: the 'friction stress', σ_f, and the 'back stress', σ_b. The friction stress corresponds to the resistance which the dislocations have to overcome to keep moving in the lattice. The back stress is associated with piled-up dislocations that were created after overcoming the friction stress.

This well-known method is illustrated in Fig. 5. At the peak stress, the applied stress σ_P is the sum of the friction stress and the back stress. On lowering the applied stress, the friction stress will oppose the backward motion of dislocations. Reversed plasticity will be obtained when the applied stress, yield stress σ_y, aided by the back stress, can overcome the friction stress. The friction stress and the back stress are simply determined as follows:

$$\sigma_P = \sigma_f + \sigma_b, \quad (2)$$

$$\sigma_y = \sigma_f - \sigma_b. \quad (3)$$

The variation of the normalized friction and back stresses with the normalized number of cycles for the unirradiated and irradiated samples is shown in Fig. 6. Due to the inaccuracy of the method, these values of stresses exhibit a scatter band which was represented by 5% of error bars in the diagram. Despite this inaccuracy, the trends of the curves are clearly defined. As shown in Fig. 6, remarkable difference of the friction stresses and the back stress behavior between unirradiated and irradiated samples is observed as cycling proceeds.

The difference of the friction stress curves could be rationalized thinking that the friction stress is difference in each cycle to the yield stress in a monotonic tensile test. It will defend on the obstacles that the initial internal structure of the metal imposes to the dislocation movement. These obstacles can be the lattice friction, precipitated particles, other dislocations and foreign atoms. As the initial structure between unirradiated and irradiated samples is considered to be very different, the yield stress for the first cycle

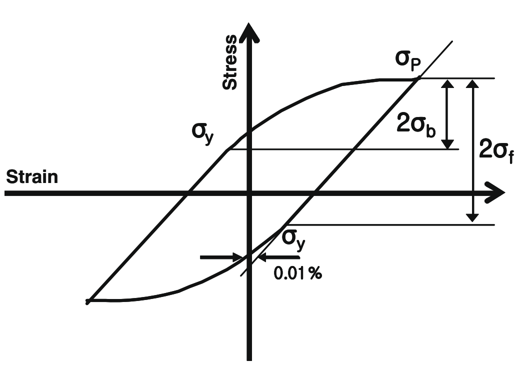

Fig. 5. Method to obtain the back and friction stresses.

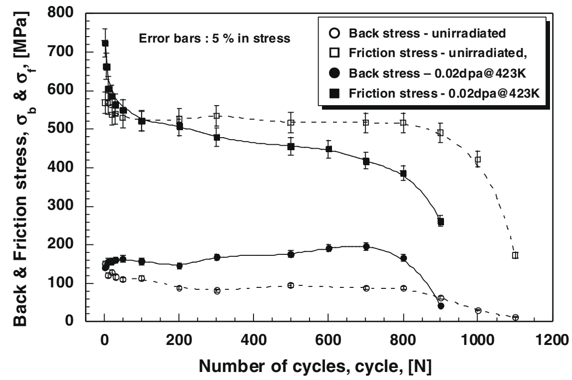

Fig. 6. Back and friction stresses with number of cycles for F82H IEA heat before and after irradiation.

(friction stress) should be different each other. In the case of neutron irradiated samples, the irradiation defects and/or defect clusters are a typical example of these obstacles which lead to polygonization in the early stage of fatigue, where the size of the polygons become smaller than those of unirradiated sample. These results should produce a larger decrease rate in the friction stress; hence, remarkable increase in cyclic softening rate occurred in the irradiated sample during LCF test.

The back stress depends on the density of long-range impenetrable obstacles that are created by the dislocations movement such as pile-ups. Therefore, the smaller the polygons produced by the irradiation defects and/or defect clusters, the larger the density of these obstacles. As a result of this effect, the back stress will be also larger. The observed increase following this initial hardening, the back stress of irradiated sample in Fig. 6, could be attributed to the increased amount of dislocations produced during cycling.

Cell structures after LCF test were observed as in the unirradiated and irradiated sample as shown in Fig. 7. Subgrain sizes of

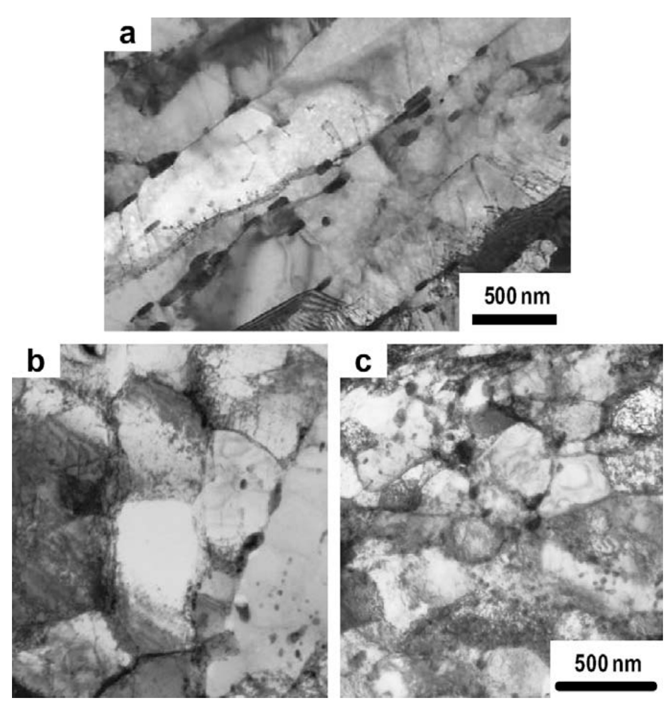

Fig. 7. TEM micrographs of cell structures observed in (a) before LCF test, (b) after LCF test with unirradiated sample and (c) after LCF test with irradiated sample.

irradiated sample were smaller than that of the unirradiated sample (compare Fig. 7(b) and (c)), and this can be correlated to the difference in the friction stress and back stress.

4. Summary

Cyclically induced softening in reduced activation ferritic/martensitic steel, F82H IEA heat, before and after neutron irradiation was investigated by cyclic stress response during LCF test at room temperature. The following conclusions were reached:

(1) The fatigue lifetimes of an irradiated sample should be shorter than unirradiated sample due to the neutron irradiation causes irradiation hardening and significant increase in cyclic softening ratio.
(2) The cyclic softening is caused by the decrease of the friction stress, and irradiated sample shows a pronounced cyclic softening rate at room temperature because the irradiation defects and/or defect clusters produce smaller polygons in the early stage of fatigue.
(3) The back stress of irradiated sample became larger than that of unirradiated sample as a result of the smaller the polygons, the larger the density of these obstacles.

References

[1] K. Shiba, M. Enoeda, S. Jitsukawa, J. Nucl. Mater. 329–333 (2004) 243–247.
[2] J. Bertsch, S. Meyer, A. Möslang, J. Nucl. Mater. 283–287 (2000) 832–837.
[3] S. Jitsukawa, A. Kimura, A. Kohyama, R.L. Klueh, A.A. Tavassoli, B. van der Schaaf, G.R. Odette, J.W. Rensman, M. Victoria, C. Pertersen, J. Nucl. Mater. 329–333 (2004) 39–46.
[4] A.F. Armas, C. Petersen, R. Schmitt, M. Avalos, I. Alvarez-Armas, N. Nucl. Mater. 307–311 (2002) 509–513.
[5] H. Tanigawa, T. Hirose, M. Ando, S. Jitsukawa, Y. Katoh, A. Kohyama, J. Nucl. Mater. 307–311 (2002) 293–298.
[6] S.W. Kim, H. Tanigawa, T. Hirose, K. Shiba, A. Kohyama, J. Nucl. Mater. 367–370 (2007) 568–574.
[7] ASTM standard E-606, Annual Book of ASTM, ASTM, 1996.
[8] M. Klesnil, P. Lukas, Fatigue of Metallic Materials, Elsevier, Amsterdam, 1980.
[9] A.H. Cottrell, Dislocations and Plastic Flow in Crystals, Oxford University, London, 1953. 111.
[10] D. Kuhlmann-Wilsdorf, C. Laird, Mater. Sci. Eng. 37 (1979) 111–120.
[11] L. Handfield, J.I. Dickson, in: G.C. Sih, Sj.W. Provan (Eds.), Defects, Fracture and Fatigue, Martinus Nijhoff, The Hague, 1983, p. 37.